Nat. Hazards Earth Syst. Sci. Discuss., 1, 4635–4680, 2013
www.nat-hazards-earth-syst-sci-discuss.net/1/4635/2013/
doi:10.5194/nhessd-1-4635-2013

Natural Hazards
and Earth System
Sciences
Discussions
Open Access

A coupling of hydrologic and hydraulic models appropriate for the fast floods of the Gardon river basin (France): results and comparisons with others modelling options

O. Laganier, P. A. Ayral, D. Salze, and S. Sauvagnargues

Ecole des Mines d’Alès, Laboratoire de Génie de l’Environnement Industriel et des Risques Industriels et Naturels, Alès, France

Received: 3 August 2013 – Accepted: 6 August 2013 – Published: 6 September 2013

Correspondence to: P. A. Ayral (pierre-alain.ayral@mines-ales.fr)

Published by Copernicus Publications on behalf of the European Geosciences Union.

Title Page
Abstract Introduction
Conclusions References
Tables Figures
|◀ ▶|
◀ ▶
Back Close
Full Screen / Esc
Printer-friendly Version
Interactive Discussion

Title Page
Abstract Introduction
Conclusions References
Tables Figures
◂◂ ▸▸
◂ ▸
Back Close
Full Screen / Esc
Printer-friendly Version
Interactive Discussion

Abstract

Mediterranean catchments are regularly affected by fast and flash floods. Numerous hydrologic models were developed, and allow to reconstruct these floods. However, these approaches often concern average size basins, of some hundreds km^2. At more important scales ($> 1000\,\mathrm{km}^2$), a coupling of hydrologic and hydraulic models appears to be an adapted solution. This study analyses the performances of a coupling of models and compares them with those of others modelling strategies. The distributed SCS-LR hydrologic model implemented in the ATHYS modelling platform (http://www.athys-soft.org), and the MASCARET hydraulic modelling code, based on full Saint-Venant equations, are employed. The coupling is applied to the Gardon river basin ($2040\,\mathrm{km}^2$), in the southeast of France. The results are satisfactory at the downstream stations. Furthermore, the coupling has few parameters, expecting interesting perspectives for flood forecasting.

1 Introduction

Fast and flash floods in the Mediterranean area are well-known for their importance and violence. They are characterized by very brutal reactions by rivers, with specific discharge rates sometimes greater than $20\,\mathrm{m}^3\,\mathrm{s}^{-1}\,\mathrm{km}^{-2}$, and flood water rising very rapidly, generally in a few hours. These reactions are the consequence of extremely rainy episodes, for which cumulated rainfall can reach values superior to 500 mm in 24 h, with intensities sometimes superior to $100\,\mathrm{mm}\,\mathrm{h}^{-1}$. In the southeast of France, the last events of this type are the ones that affected the Aude river in November 1999 (Gaume et al., 2004), the Gard area in September 2002 (Delrieu et al., 2005), and the Var area in June 2010 (Martin, 2010). Each of these events took many human lives, and generated damage of more than 1 billion euros.

In the literature, studies indicate a whole range of satisfactory solutions for flash flood modelling, although there is not, at the moment, a clear consensus as to a preferential approach (Hapuarachchi et al., 2011). This modelling research generally concerns average size catchments, often smaller than a few hundred km^2. Likewise, in the case of the Gardon river basin in the southeast of France, which was strongly impacted by the extreme event of September 2002, the literature proposes numerous assessments of hydrologic models adapted to these small scales. Many of these studies concern the *Gardon d'Anduze* sub-catchment (545 km^2), for which discharge data are particularly complete (see for example: Bouvier et al., 2004, 2006; Ayral et al., 2005; Marchandise, 2007; Moussa et al., 2007; Toukourou et al., 2010; Roux et al., 2011; Thierion et al., 2011; Tramblay et al., 2011), or smaller sub-catchments (see for example: Estupina-Borrell and Dartus, 2003; Manus et al., 2009; Anquetin et al., 2010; Braud et al., 2010; Tramblay et al., 2010; Artigue et al., 2012).

While the hydrologic modelling of sub-catchments is well informed, the literature is much less complete in terms of modelling applied to the complete area of large Mediterranean catchments (> 1000 km^2). This lack of knowledge is surprising, because the most extreme events often concern these large areas. For the September 2002 extreme event in the Gard area, cumulated rainfall exceeded 200 mm in 24 h all over a 5500 km^2 area (Delrieu et al., 2005). However, as far as we know, at the Gardon river basin scale (2040 km^2), only the research of Bonnifait et al. (2009) can be cited. At this scale, hydrologic models are difficult to apply a priori, because they are based on conceptualization of routing streamflows that is often simplified. Other approaches must be used, such as the combination of hydrologic and hydraulic models (Claudet and Bouvier, 2004). This is the approach chosen by Bonnifait et al. (2009), and which is also used in our research.

As Lerat et al. (2012) indicate, couplings of hydrologic and hydraulic models are not very frequent in the literature. The studies often concern applications of these couplings to different kinds of cases (see for example: Knebl et al., 2005; Whiteaker et al., 2006; Lian et al., 2007; Biancamaria et al., 2009; Bonnifait et al., 2009; Montanari et al., 2009; Mejia and Reed, 2011). To our knowledge, few studies propose sensitivity analysis based on coupled models, in particular to upstream and lateral inflows. Lerat et al. (2012) give an example, applied to the Illinois River (USA).

The main objective of this study is to assess the performance of coupling hydrologic and hydraulic models applied to the Gardon river basin (2040 km^2). Our research is based on significant already existing hydrologic modelling of the sub-catchments of the site studied. The coupling analysed is based on a very simple parameter adjustment strategy, making it possible to foresee future operational use. The following two questions are analysed in particular:

- What is the performance of the coupled models? The goal is to estimate the quality of the hydrologic modelling of upstream inflows, lateral inflows, and how the coupled model performs in the intermediate-downstream part of the basin.

- How does this kind of performance compare with other modelling or coupling options? A three-way comparison is made between the results when only the hydrologic model is used, which is extended to the downstream part of the catchment, and when only the hydraulic model is used (without lateral inflows), and when there is a coupled model taking account of the inflows observed or modelled upstream.

The coupling of models was assessed for various events, with rather different characteristics. Rainfall radar data and discharge data from five stations were used.

This article is organized as follows. Part two provides a description of the Gardon catchment, the hydrologic data used, and the events studied. Part three describes the strategy for implementing the coupling approach, the hydrologic and hydraulic models, and the parameters adjustment. Finally, the article ends with a discussion and a description of the results.

2 Study area and flood events modelled

2.1 The Gardon catchment

The Gardon River is a major tributary of the downstream part of the Rhône River, located in the southeast of France (Fig. 1). Its watershed area is 2040 km^2 at the confluence. The source of the Gardon River is in the Cevennes, a low mountain range with a 1699 m peak, the *Pic Cassini*. It contains two main upstream reaches, the *Gardon d'Alès* and the *Gardon d'Anduze*, and a single downstream reach. The *Gardon d'Alès* and *Gardon d'Anduze* meet a few kilometres upstream from the village of Ners, in the intermediate part of the catchment.

The upstream and downstream parts of the Gardon river basin have very different features. In the upstream part, the river system has many branches, and a landscape with steep-sided valleys and steeply-sloped hillsides. In some places, slopes are greater than 50 %. From a geological point of view, this area is essentially made up of former grounds of primary age, with a preponderance of schist and granites, and a lower proportion of sandstone. The vegetation consists of oaks and chestnut trees, with a great number of conifers at high altitude. Downstream from Alès and Anduze, the valleys widen and create alluvial plains with deposits of the Quaternary, which in some places extend over several kilometres. The widest point is in the *Gardonnenque* plain. The river system is simplified, because it crosses softer formations of the secondary era (limestone, marls, and sandstone). Some elements of relief remain, which rarely exceed 200 m. The landscape is dominated by scrubland and cropland. This zone of plains ends with the Gardon gorges, which are profoundly dug in limestone, and in some places rise up to about 100 m. The Gardon gorges stretch over about twenty kilometres. The River Gardon tributaries have a highly karstic nature in these places. Downstream from the gorges, the River Gardon crosses a zone of alluvial deposits from the River Rhone. The floodplain widens, although less than in the *Gardonnenque* plain.

There are some moderate size cities (Fig. 1) in this catchment, which is predominantly rural. Located in the intermediate part of the catchment, Alès is the biggest city with a current population of slightly more than 40 000 inhabitants. Total population in the catchment was estimated to be 191 000 inhabitants in 2006 (orig.cg-gard.fr), of which about 25 % live in flood risk areas.

Climate in the Gardon watershed is typically Mediterranean. It is characterized by sometimes very intense and violent rainy events, which generally occur in the autumn. These events cause fast floods (flash floods in the upstream parts), which sometimes have tragic consequences. The catastrophic event in September 2002, which affected the River Gardon and the nearby Cèze and Vidourle river basins, is still in everyone's mind. Values cited in the literature demonstrate how exceptional it was (Delrieu et al., 2005). Cumulated rainfall between 600 and 700 mm in 24 h was observed in the triangle linking the cities of Alès, Anduze, and Ners, which is the current record in the region. Peak specific discharges superior to 20 $\mathrm{m^3\,s^{-1}\,km^{-2}}$ were recorded in certain sub-catchments (Delrieu et al., 2005). There were 23 victims, and damage was estimated to be 1.2 billion euros for the whole area (Sauvagnargues-Lesage and Simonet, 2004; Ruin et al., 2008).

2.2 Hydrological data and events studied

Discharge data from five hydrometric stations in the catchment were used. Figure 1 indicates the locations of these stations. Table 1 provides data on the surface area drained and the catchment outlet distances for each station. Rainfall radar images at 1 km resolution were also analysed. They come from two Météo-France radars, located near the catchment, in the cities of Bollène and Manduel (Fig. 1). The radar images were corrected beforehand according to the rain gauge network measurements, using CALAMAR® software (Ayral et al., 2005; Thierion et al., 2011). These discharge and rainfall data were supplied by the regional flood warning service SPC-GD ("*Service de Prévision des Crues Grand Delta*"), and have a 5 min time step. This fine time step is used for modelling, as it is well adapted to the fast kinetics of events in this catchment.

For this study, seven events were analysed, which occurred between 2005 and 2011. These events were among the most important ones during the period, for which hydrological data are the most complete. Table 2 summarises some of their characteristics. Total rainfall upstream to Russan varied between 135 mm for event no. 6 and 372 mm for event no. 7. Peak flows in this station were between 700 $m^3 s^{-1}$ (event no. 5) and 1420 $m^3 s^{-1}$ (event no. 4). Figure 2 provides data for the cumulated rainfall distribution in the catchment for each event. Two general trends can be seen:

- For events no. 1 and 5, cumulated rainfall is more significant in the intermediary-downstream part of the catchment. Table 2 shows for these two cases an increase in the volume at the downstream stations, indicating the proportionally important contribution of lateral inflows in these zones.
- For events no. 2, 3, 4, 6, and 7, cumulated rainfall was more important in the upstream part of the catchment. This distribution of rain is the one most frequently observed (Météo-France, 1996), because the Cevennes mountains amplify the rainfall. The volume increased between the upstream stations and the station of Ners, in a way, however, rather different according to the event. Lateral inflows were the most important for events no. 6 and 7. Volumes diminished between Ners and Russan for events no. 2, 3, and 4. This decrease can be understood in terms of karstic losses in the river bed, and also corresponds to insignificant contributions of lateral inflows between both stations.

Some remarks concerning the hydrological data of these events must be made. Hydrographs at the Alès station are not available for events no. 1 and 2, because the station rating curve is not valid for these periods. The rating curve at Remoulins is very uncertain, and its discharge data were not used in this study. Finally, in the case of event no. 6, rainfall radar data are missing at the beginning of the event. They were completed by rain gauge measurements using inverse distance interpolation techniques.

3 Modelling strategies

3.1 Coupling used

An external and unidirectional coupling of models was used for this study, as defined by Lian et al. (2007), and Mejia and Reed (2011). In this type of coupling, both models function independently. In the first phase, upstream and lateral inflows to the hydraulic model are evaluated using hydrologic modelling. Then, hydraulic modelling integrating these inflows is conducted. In this way, the hydraulic model does not interact with the hydrologic model, which involves some simplifications of what really exists: for example, backwater effects on tributaries are neglected. It is the most common coupled approach generally chosen, because it is simple to implement and flexible, the use of other models which can be so easily envisaged (Whiteaker et al., 2006). This last criterion is particularly well adapted to our study, because the literature does not indicate a clear consensus on the preferential approach for hydrologic modelling of flash flood catchments (Hapuarachchi et al., 2011). An example of this type of coupling applied to the Gardon river basin in the case of the September 2002 extreme event was proposed by Bonnifait et al. (2009). Other studies concern catchments in various hydrometeorological contexts (Knebl et al., 2005; Whiteaker et al., 2006; Lian et al., 2007; Biancamaria et al., 2009; Mejia and Reed, 2011).

Figure 3 shows how the coupled model was implemented in the catchment area studied. The hydraulic model is applied from the Anduze and Alès stations up to the Remoulins station. This reach was chosen because the floodplain widen considerably downstream from both upstream stations, leading to important overflowing during strong floods. It includes the gorges zone, which is very influential during extreme events.

The hydraulic model consists of three reaches. Both upstream reaches correspond to the downstream parts of the *Gardon d’Anduze* and *Gardon d’Alès*, which are 14.5 and 12.5 km long. The downstream reach connects the confluence with the Remoulins station, and is 55.2 km long. The total extent of the hydraulic model is 82.2 km. There are about 50 inflows, with two major upstream inflows (the Alès and Anduze sub-catchments), and 48 lateral inflows (Fig. 3). Lateral inflows were defined on the basis of a minimum threshold area of 1 km^2. The average area of lateral sub-catchments is 20 km^2, for a median value of 5 km^2. Sub-catchments no. 2, 20, 26, 28, and 39 have an area greater than 50 km^2, the maximum being 203 km^2 for inflow no. 39. All in all, the selected lateral sub-catchments cover 92 % of the area between both upstream stations and the Remoulins station.

The coupling uses the SCS-LR hydrologic model implemented in the ATHYS modelling platform (http://www.athys-soft.org), and the MASCARET one-dimensional hydraulic modelling code. The ATHYS platform is developed by the IRD ("*Institute of Research for Development*"), and the MASCARET code by EDF ("*Electricité De France*" – French Electric Company), and the CETMEF ("*Centre d'Etudes Techniques Maritimes et Fluviales*"). Both tools, which will be described in the following section, are open-source.

3.2 The models coupled

3.2.1 SCS-LR hydrologic model

The SCS-LR model combines a runoff model adapted from the Soil Conservation Service (SCS) and a Lag and Route model (LR). It is an events-based, distributed model with reservoirs, based on a grid of regular square cells. It has been used in many studies on Mediterranean watersheds of limited area, in particular concerning the *Gardon d'Anduze* river basin (Bouvier et al., 2004, 2006; Marchandise, 2007; Tramblay et al., 2011). It proves to be successful for modelling typical floods on Mediterranean watersheds, particularly compared with other models (Bouvier et al., 2006; Marchandise, 2007; Coustau, 2011).

The SCS runoff model associates a time variable runoff coefficient $C(t)$ with every grid cell, which depends on the cumulated rainfall $P(t)$, and on an S parameter, characterising the initial water deficit in the catchment area:

$$C(t) = \left(\frac{P(t) - 0.2S}{P(t) + 0.8S}\right)\left(2 - \frac{P(t) - 0.2S}{P(t) + 0.8S}\right) \tag{1}$$

with $P(t)$ and S in mm, $C(t)$ in %.

This runoff coefficient increase with the cumulated rainfall. To represent its decrease during period without rains, a reduction of $P(t)$ is added:

$$\frac{\mathrm{d}P(t)}{\mathrm{d}t} = Pb(t) - dsP(t) \tag{2}$$

where $Pb(t)$ is the instantaneous precipitation in mm h^{-1}, and ds a coefficient [t^{-1}].

Finally, the runoff $R(t)$ of the cell (mm h^{-1}) is expressed as:

$$R(t) = C(t) \cdot Pb(t) \tag{3}$$

The LR routing model is based on the definition of a propagation time T_m and of a diffusion time K_m for each cell m, estimated from the cell to outlet distances l_m:

$$T_m = \frac{l_m}{V_0} \tag{4}$$

$$K_m = K_0 T_m \tag{5}$$

where V_0 is the speed of propagation (m s^{-1}), and K_0 a coefficient without dimension. The elementary discharge $q(t)$ at outlet, corresponding to the propagation of the runoff $R(t_0)$ generated at the cell m at time t_0, is:

$$\begin{aligned} &q(t) = 0 \\ &\text{if } t < t_0 + T_m \\ &q(t) = \frac{R(t_0)}{K_m}\exp\left(-\frac{t-(t_0+T_m)}{K_m}\right)B \\ &\text{if } t > t_0 + T_m \end{aligned} \tag{6}$$

where B is the cell surface.

Finally, the complete flood hydrograph is obtained by adding all the contributions of the cells, at each time. A five-minute time step is used for modelling.

This model is a simplified version of the complete SCS-LR model of the ATHYS platform, and is identical to the one used by Tramblay et al. (2011). The simplification concerns the SCS runoff model, for which the contribution of delayed flows was ignored. This version gave good results at the Anduze station, for 16 events (Tramblay et al., 2011). Besides this last observation, it was chosen because it has a low number of adjustment parameters (see Sect. 3.3).

The cell grid was defined with the help of a Digital Elevation Model (DEM) on the basis of the IGN's BD ALTI® ("*Institut national de l'information géographique et forestière*"). The cell size is of 100 m × 100 m. This resolution is particularly well adapted to the smallest lateral sub-catchments. The flow paths between each cell, allowing the propagation and diffusion times to be evaluated, were forced according to the river polylines of the catchment, on the basis of the IGN's BD CARTHAGE®. This processing seemed necessary in the intermediate-downstream part of the Gardon catchment, where low slopes falsify flow paths, and the areas really drained.

The rainfall radar data at 1 km resolution were interpolated in each cell according to the Thiessen method. This choice of spatially distributed rainfall information is justified by the literature, the performances of various models are clearly improved in Mediterranean catchments (Saulnier and Le Lay, 2009; Sangati et al., 2009; Anquetin et al., 2010; Zoccatelli et al., 2010; Tramblay et al., 2011).

3.2.2 The MASCARET hydraulic model

MASCARET is the one-dimensional hydraulic modelling code used for developing the hydraulic model. It can be used to calculate steady and unsteady flows in fluvial and transcritical systems. It is based on full Saint-Venant equations, composed of the continuity equation:

$$\frac{\partial Q}{\partial x}+\frac{\partial A}{\partial t}=q_l \tag{7}$$

and of the dynamic equation:

$$\frac{\partial Q}{\partial t}+\frac{\partial}{\partial x}\left(\beta\left(x,A\right).\frac{Q^2}{A}\right)+gA\left(\frac{\partial Z}{\partial x}+J\right)=0 \tag{8}$$

where Q is the discharge ($\mathrm{m^3\,s^{-1}}$), x the longitudinal distance (m), A the wetted area ($\mathrm{m^2}$), q_l the lateral inflows by meter ($\mathrm{m^2\,s^{-1}}$), β the Boussinesq coefficient, without dimension, characterizing the variations of speed in the cross-section, g the gravity, Z the elevation of surface (m), and J the linear friction losses. Using the Manning–Strickler expression, J can be written:

$$J=\frac{Q^2}{K_\mathrm{s}^2A^2R_\mathrm{h}^{4/3}} \tag{9}$$

with K_s the Strickler coefficient ($\mathrm{m^{1/3}\,s^{-1}}$) which characterizes roughness, and R_h the hydraulic mean radius (m) such as $R_\mathrm{h}=A/P$, with P the wetted perimeter (m).

The Saint-Venant equations are valid for streams of weak slopes (lower than 10 %), and when the flow follows a privileged direction. Furthermore, they imply hypotheses of hydrostatic pressure and of constant density of water. In the face of hydraulic structures (weirs, dams...), they are replaced locally by the corresponding hydraulic equations (EDF-CETMEF, 2011). Numerical techniques are used to the resolution. Two schemes, explicit and implicit in time, are implemented in the MASCARET code, and are at the user choice.

As indicated above, the hydraulic model contains three main reaches (Fig. 3), connected by a zone of confluence. The topographic data provided concern river cross sections. They are identical to those in the study by Bonnifait et al. (2009). These data were collected with the SPC-GD and the SMAGE ("*Syndicat Mixte d'Aménagement des Gardons*"). Missing in the gorges sector, the authors had to complete them by means of 1 : 25 000 maps. All in all, the hydraulic model used contains 161 cross sections, with an average spacing of 530 m.

The initial condition of the hydraulic model is a water line, characterizing the base flow. In this study, it is identical for all the events, and corresponds to a constant discharge of 5 $m^3 s^{-1}$ injected into both upstream stations. The parameters adjusted in the model are Strickler coefficients, which differ in the river bed and in the floodplain.

The explicit scheme is used for the resolution, requiring a very fine time step, of 0.1 s in this studied case. The model results are then sampled at 5 min for the analysis.

3.3 Model parameter adjustments

A very simplified approach for hydrologic model parameter estimation was chosen. Only the S parameter of the runoff model defined previously, and V_0, speed of propagation associated with the LR routing model, are calibrated for each event. This low number of parameters limits equifinality problems linked to the calibration procedure, and is in theory better adapted to a transposition to ungauged catchments (lateral inflows). Other model parameters were set for all the events, and the values determined by Tramblay et al. (2011) on the *Gardon d'Anduze* river basin were used (i.e., $ds = 0.4$ and $K_0 = 1.5$).

Both parameters, S and V_0, were calibrated at Anduze, for each event. They were then used for the modelling of the second upstream catchment (Alès), and for those of the 48 lateral inflows. The data from the Alès station were only considered as an indicator of the validity of transposing parameters. The hydrologic model parameters were calibrated at Anduze with the simplex iterative algorithm (Nelder and Mead, 1965), implemented in the ATHYS platform. The well-known Nash criterion (Nash and Sutcliffe,

1970) was employed for the calibration procedure:

$$\text{Nash} = 1 - \frac{\sum_{i=1}^{T}(Q_{\text{OBS},i} - Q_{\text{MOD},i})^2}{\sum_{i=1}^{T}(Q_{\text{OBS},i} - \overline{Q_{\text{OBS}}})^2} \tag{10}$$

where T is the event duration, and $Q_{\text{OBS},i}$ and $Q_{\text{MOD},i}$ ($\text{m}^3\,\text{s}^{-1}$) are the observed and modeled dicharges at time step i.

The calibration domain includes only discharges superior to $50\,\text{m}^3\,\text{s}^{-1}$, to limit the influence of low values. However, in the case of event no. 5, for which peak flow does not reach this threshold at Anduze (Table 2), the calibration procedure was applied to discharges superior to $10\,\text{m}^3\,\text{s}^{-1}$.

Table 3 indicates the parameter values calibrated at Anduze for the 7 events studied. The S parameter value follows a coherent trend. For events arising just after the summer season, the S parameter is high, characterising an important water deficit. On the contrary, for events in November–December, the values are lower, since rainy events at the beginning of autumn have contributed in a more or less significant way to refilling the catchment. The performance of the hydrologic modelling is described in Sect. 4.1.1.

The K_s Strickler coefficients of the hydraulic model were empirically adjusted. The procedure consisted in reducing as much as possible the time differences between the observed and simulated peaks, and between the observed and simulated beginning of flood rises, at the three stations in Ners, Russan, and Remoulins. The beginning of the flood rise is identified as the first discharge value exceeding $50\,\text{m}^3\,\text{s}^{-1}$. Several sets of the Strickler coefficient were estimated, for which values vary from 15 to 30 in the river bed, and from 10 to 15 in floodplain. The adjustment procedure was applied to event no. 3. The hydrographs observed at Anduze and Alès, and the lateral inflows modelled are the boundaries conditions of the hydraulic model. This event was chosen because the lateral inflow contributions were weak (Tab. 2), and had little influence in terms of shifting the peak times.

The best set considered a Strickler coefficient of 25 in the river bed, except in the gorges, where it was 30, and 10 in the floodplain. This parameterisation is very satisfactory in terms of peak flow timing. The peak modelled for event no. 3 was 5 min late at Ners, 5 min early at Russan, and on time at Remoulins. The peak propagation times from one station to another seem to be entirely satisfactory. Performance was a bit less satisfactory concerning the beginning of flood rise times, with an average delay of one hour at the three stations. This parameter set was used for all the other events in the study.

In this way, only two parameters in the coupled models were adjusted for each event, at the Anduze station. Other parameters and initial conditions remained identical. This parsimonious criterion makes the coupling very interesting from an operational point of view.

3.4 Performance assessment

The performance of the coupled models was evaluated by analysing discharge data from five stations in the catchment area, as indicated in Sect. 2.2. The quality of the hydrologic modelling was estimated on the basis of hydrographs recorded at Anduze and Alès, and for lateral inflows according to the differences in volume observed between two consecutive stations. The performance of the coupling was evaluated at three stations in the downstream part of the catchment (Ners, Russan, and Remoulins).

Three quality indicators were assessed. First, the Nash coefficient, which was already mentioned in the last section. It provides information on the overall quality of the hydrographs modelled. The other two indices are specific to peak flow. These coefficients are the relative error for peak flow $\mathrm{RE}_{\mathrm{Qm}}$ (%), and the temporal difference between the observed and simulated peaks ΔT_{Qm} (min):

$$\mathrm{RE}_{\mathrm{Qm}} = \frac{\mathrm{Qm}_{\mathrm{MOD}} - \mathrm{Qm}_{\mathrm{OBS}}}{\mathrm{Qm}_{\mathrm{OBS}}} \times 100 \tag{11}$$

$$\Delta T_{\mathrm{Qm}} = T_{\mathrm{MOD}} - T\mathrm{m}_{\mathrm{OBS}} \tag{12}$$

with $\mathrm{Qm}_{\mathrm{MOD}}$ and $\mathrm{Qm}_{\mathrm{OBS}}$ as the modelled and observed peak flows ($\mathrm{m}^3\,\mathrm{s}^{-1}$), and $T\mathrm{m}_{\mathrm{MOD}}$ and $T\mathrm{m}_{\mathrm{OBS}}$ as the corresponding times. A positive $\mathrm{RE}_{\mathrm{Qm}}$ value indicates an overestimation in the peak modelled, and conversely. The ΔT_{Qm} index is positive when the peak modelled is late, and negative if it is early. At the Remoulins station, only the ΔT_{Qm} index was estimated, because the rating curve was too uncertain as indicated above.

4 Results

4.1 Coupled model results

4.1.1 Hydrologic modelling of upstream inflows and lateral inflows

The SCS-LR hydrologic modelling results were evaluated at both the Anduze and Alès stations, and for lateral inflows according to the differences in volumes observed between the downstream stations.

Table 4 presents the modelling results at Anduze (the calibration station) and Alès. Events no. 1 and no. 2 were not provided for the second station, because the rating curve was not valid during these periods (see Sect. 2.2). Performance was generally satisfactory at Anduze, with Nash values varying from 0.53 to 0.91. A similar range of values was observed by Tramblay et al. (2011) with the same version of the model, for a 16 event set at Anduze. At the Alès station, Nash values were very different from one event to another, indicating qualities varying from very bad to very good. The Nash

Title Page
Abstract Introduction
Conclusions References
Tables Figures
◀I ▶I
◀ ▶
Back Close
Full Screen / Esc
Printer-friendly Version
Interactive Discussion

index decreased for all events compared with the Anduze values. The peak evaluation indices were, however, rather satisfactory at both stations. Peak error was between 0 and ±25 %, and the ΔT_{Qm} index between 0 and ±30 min, for 5 events. Only events no. 6 and no. 7 present major errors. These two cases contain several peaks, and a secondary peak was identified as the main peak by the model. Some hydrographs modelled at Anduze and Alès are represented in Fig. 4. Flood fall is in general rather poorly represented, particularly for winter or end of autumn events. This observation is directly attributable to the choice of a simplified version of SCS-LR model.

Table 5 compares the differences in volumes observed between the downstream stations, with the volumes generated by lateral inflows included between these stations, estimated with SCS-LR. The differences in volumes at Ners cannot be estimated for events no. 1 and 2, and the hydrographs at Alès were missing as indicated above. There appears to be a tendency to underestimate the volumes modelled for lateral inflows along the Alès/Anduze–Ners reaches, and on the contrary a tendency to overestimate them for those along the Ners–Russan reach. There is volume compensation at the Russan station, where the total volume modelled for lateral inflows since Alès and Anduze is closer to the differences in volumes observed, than at the Ners station. It is difficult to propose a physical interpretation of these inflow differences between both sections. The rather marked karstic functioning of the downstream sub-catchments, for which the hydrologic model is not in theory well adapted, and the uncertainties linked to the rating curves, are possible explanations.

4.1.2 Coupling performance at the downstream stations

The results of the coupled models at the Ners, Russan, and Remoulins stations are presented in Table 6. Coefficients are generally good for the selected range of events. The Nash index is between 0.61 and 0.92 at Ners, and between 0.72 and 0.97 at Russan. Event no. 3 presents the highest values at both stations, whereas event no. 2 has the lowest. The $\mathrm{RE}_{\mathrm{Qm}}$ index has satisfactory values between 0 and ±15 % for most events. However, peaks for events no. 1, 5, and 7 at the Ners station, present more important errors, with the highest peak overestimation of 39 % for event no. 7. The ΔT_{Qm} index was equal to or less than 30 min for five events at Ners, and for four at Russan and Remoulins, which characterises good peak flow timing, and confirms the hydraulic model parameterisation described in Sect. 3.3. However, this coefficient is very high at three stations for event no. 7: the delay for the peak modelled is more than twenty hours.

Results presented in Table 6 also bring to light an improvement in the Nash values at Russan, compared with those at Ners, for all events. The average increase was 13 % between both stations. There is a twofold explanation for this observation. First, the improvement in the modelling of events no. 2, 3, and 4 (varying from +0.05 to +0.11) for which lateral inflows at the section Ners–Russan are insignificant or of little importance (Table 5), indicate that the hydraulic model is better adapted at Russan, and/or a more valid rating curve at this station. It is necessary to specify that the Ners station is located only 4 km downstream from the confluence, which complicates the hydraulic model. It is also possible that the topographic data of the hydraulic model are more precise near Russan. The second explanation concerns the others events, and particularly those for which lateral inflows are proportionally important (events no. 1 and no. 5). It was previously noted that the total volume of lateral inflows from Alès and Anduze is more satisfactory at Russan than at Ners, as there is a compensation at the most downstream station. This more correct estimation also seems to be responsible for the improved results of the coupled models at Russan. The Nash values increased for events no. 1 and 5 by +0.09 and +0.20. If this trend toward improvement is clear for the Nash coefficient, it is barely obvious for the indices concerning peak flow.

4.2 Comparison with other modelling strategies

The results of the coupled models presented above are now compared with those of other modelling options. The differences between these options concern the addition of lateral inflows (simple hydraulic model or coupling), the upstream inflows (observed or modelled hydrographs), and the routing conceptualization.

For more clarity, the abbreviation $\mathrm{COUPL_{MOD}}$ identifies the coupled models used previously. The following other modelling options were assessed:

- Option no. 1: only the SCS-LR hydrologic model is used. This option differs from $\mathrm{COUPL_{MOD}}$ in terms of routing considerations downstream from Alès and Anduze, concerning the representation of the river bed, and the equations solved. Upstream inflows and lateral inflows were identical. This option is identified as SCS-LR.
- Option no. 2: only the hydraulic model is used, without lateral inflows. As for $\mathrm{COUPL_{MOD}}$, upstream inflows were the hydrographs modelled. This option is expressed as $\mathrm{SV_{MOD}}$.
- Option no. 3: identical to the previous one, but upstream inflows were the hydrographs recorded. This approach is expressed as $\mathrm{SV_{OBS}}$.
- Option no. 4: is identical to the previous one, but lateral inflows are added. In other words, the differences with $\mathrm{COUPL_{MOD}}$ concern only hydrographs at upstream inflows, and the observed data were taken into consideration. This option is expressed as $\mathrm{COUPL_{OBS}}$.

As mentioned above, the hydrographs recorded are not available at the Alès station for events no. 1 and 2. The hydrographs recorded at Anduze and modelled at Alès are taken into account for the $\mathrm{SV_{OBS}}$ and $\mathrm{COUPL_{OBS}}$ options in these two cases.

Figure 5 illustrates the differences in the Nash indices estimated at the Ners and Russan stations, according to the options tested. These results are analysed in the following sections.

4.2.1 SCS-LR results

Except for events no. 1 and 5, the performance of SCS-LR was among the worst at both stations, especially at Russan (Fig. 5). The Nash values vary from 0.46 to 0.93

at Ners, and from 0.52 to 0.86 at Russan. Compared with the $COUPL_{MOD}$ results, the Nash index is lower on average by 10 % at Ners and 17 % at Russan.

There is an accentuation of differences between both options downstream. This accentuation results from the improvement in the performance of $COUPL_{MOD}$ at Russan, described above, and from quality losses from SCS-LR. In fact, the Nash indices for five events decrease between both stations when SCS-LR is used.

Figure 6 compares the hydrographs of events no. 3 and 5, modelled with SCS-LR and $COUPL_{MOD}$. For event no. 3, the Nash indices according to both options are equal at Ners (excellent values of 0.93), but clearly differ at Russan (0.97 with $COUPL_{MOD}$ vs. 0.80 with SCS-LR). Differences are important in the case of event no. 5, the coefficient values were 30 % superior for the coupling at both stations. The hydrographs in Fig. 6 also indicate a general trend observed for all events when SCS-LR is used: flood peaks are underestimated, and a spreading of hydrographs is observed.

These observations show that a simplified hydrologic routing scheme is not adapted to the downstream part of the Gardon River, and confirm the results of previous studies for other catchments (Lian et al., 2007; Mejia and Reed, 2011), or for the Gardon river basin (Bonnifait et al., 2009).

4.2.2 Interest of adding lateral inflows

The interest of adding lateral inflows is extremely variable from one event to another, as shown in Fig. 5. It seems to depend on the cumulated rainfall spatial distribution of each event (Fig. 2). So, in the case of events no. 2 and 3 for which rainfall was more substantial in the upstream part, the Nash indices are almost identical for the SV_{OBS} and $COUPL_{OBS}$ options, and for the SV_{MOD} and $COUPL_{MOD}$ options. A maximum improvement of 2 % in the coefficient was observed at the Russan station for event no. 3. This fact was expected because the lateral inflows modelled are of little importance for these two events (see Table 5).

More significant improvements are noticed for events no. 4, 6, and 7. These events present more significant cumulated rainfall in the upstream part of the catchment, but also a substantial amount downstream (Fig. 2). For example, the Nash coefficients improved from 4 to 23 % at both stations, between the $\mathrm{SV_{OBS}}$ and $\mathrm{COUPL_{OBS}}$ options. This fact demonstrates the real interest of adding lateral inflows for these three events. The most significant increases in the index are noted for event no. 6, for which lateral inflows are rather consequent (Table 5). The comparison of the $\mathrm{SV_{MOD}}$ and $\mathrm{COUPL_{MOD}}$ options indicates identical improvement for events no. 4 and 6. For event no. 7, lower quality was observed when lateral inflows were taken into consideration. The Nash coefficient obtained with the $\mathrm{SV_{MOD}}$ option decreased by 7 % at the Ners station and 9 % at Russan. This decrease can be explained in terms of the hydrologic modelling errors at Alès and Anduze: the second peak in this event was rather significantly overestimated at both upstream stations (see Sect. 4.1.1). The addition of lateral inflows amplifies these errors downstream, and as a consequence modelling is of lower quality. This case of lower quality was the only one observed when lateral inflows were added.

Concerning events no. 1 and 5, for which cumulated rainfall was more substantial in the intermediary-downstream part of the catchment, improvements were very significant. For example, the Nash values increased from −0.73 for $\mathrm{SV_{MOD}}$ to 0.88 for $\mathrm{COUPL_{MOD}}$ in the case of event no. 5 at Russan. Significant improvements in the values and time of peaks were also observed. These observations reveal the need to take into consideration lateral inflows in these two cases.

Figure 7 shows the hydrographs obtained with the $\mathrm{SV_{OBS}}$ and $\mathrm{COUPL_{OBS}}$ options for events no. 1, 3, 6, and 7 at Russan. As indicated above, the addition of lateral inflows improves very clearly the modelling of event no. 1, and on the contrary has little influence on event no. 3. In this case, a better peak flow estimation was, however, observed when lateral inflows were taken into consideration. For event no. 6, the $\mathrm{SV_{OBS}}$ option underestimates rather significantly the main peak observed, and there was a better estimation of the peak with $\mathrm{COUPL_{OBS}}$.

Finally, adding lateral inflows improves the quality of the modelling in the downstream part in most of cases. This improvement depends on the cumulated rainfall spatial distribution of the event. However, deterioration is observed for event no. 7, being understandable by an increase of the errors already observed at both upstream stations.

4.2.3 Interest of options with the upstream inflows observed

The SV_{OBS} and $COUPL_{OBS}$ options take into account the hydrographs recorded for both upstream inflows.

The comparison of the SV_{OBS} and SV_{MOD} options, and $COUPL_{OBS}$ and $COUPL_{MOD}$ options shows, as in the previous point, extremely variable improvements according to the events (Fig. 5). Events no. 1 and 5 were not very sensitive, and the index varied little when the upstream hydrographs recorded were taken into consideration. For example, for event no. 1, the Nash index is equal at Ners for the $COUPL_{OBS}$ and $COUPL_{MOD}$ options, and shows an insignificant increase of +0.01 at Russan. This observation can be explained in terms of the minor importance of the upstream inflows compared to the lateral inflows for these two events. The quality of the modelling of the upstream inflows is very clearly of little importance.

The observation is different for others events. The improvement of the index between the $COUPL_{OBS}$ and $COUPL_{MOD}$ options was between 12 % and 48 % for events no. 2, 4, 6, and 7 at Ners and Russan. A more limited increase was observed for event no. 3, of 4 % at Ners, and 2 % at Russan. For these five events, the improvements observed seem to be dependent on the quality of the modelling of the upstream inflows in the hydraulic model (Table 4). Logically, when the Nash values are high at both upstream stations, the downstream differences are small. This was for example the case for event no. 3. On the contrary, for lower upstream performance, the difference is more important. For example, event no. 6 returned an average Nash value at Anduze (0.68), and a very bad one at Alès (−0.50), resulting in strong increases between the $COUPL_{OBS}$ and $COUPL_{MOD}$ options at Ners (0.64 vs. 0.95) and at Russan (0.73 vs. 0.95). This observation raises an interesting point. For events no. 6 and 7, it seems that the very bad performance at Alès ultimately had little influence on the $COUPL_{MOD}$ results at Ners and Russan (Table 5). This can be partially explained by the smaller contribution of the Gardon d'Alès in terms of volume. For example, for event no. 6, the volumes modelled at Alès and Anduze represent 24 % and 49 % of the volume modelled at Russan. A parallel can be made with one of the results of the study of Lerat et al. (2012). For the various coupling configurations tested out, these authors showed there is greater sensitivity of the modelling quality of a tributary, than for stations located on the main channel.

Some hydrographs modelled with the $\mathrm{COUPL_{OBS}}$ and $\mathrm{COUPL_{MOD}}$ options are given in Fig. 7. Nash indices are quasi-equal in the case of event no. 1 (0.88 and 0.89), with a very small improvement for event no. 3 (0.97 with $\mathrm{COUPL_{MOD}}$ vs. 0.99 with $\mathrm{COUPL_{OBS}}$), and an important increase for event no. 6 (0.73 with $\mathrm{COUPL_{MOD}}$ vs. 0.95 with $\mathrm{COUPL_{OBS}}$). For this last case, the peak flows modelled were, however, equal at this station.

Finally, Fig. 5 shows higher Nash indices with the $\mathrm{SV_{OBS}}$ option compared to $\mathrm{COUPL_{MOD}}$ for events no. 2, 3, 4, 6, and 7. This fact indicates that for these kinds of events it is better to conduct high quality modelling for the upstream inflows, rather than adding lateral inflows. The differences are particularly important for events no. 2, 4, 6, and 7, which were between 12 % and 34 % at the Ners station. However, differences were less important at Russan. The total volume of lateral inflows was more important since both upstream stations, and compensated for the modelling errors at Alès and Anduze. So, for event no. 6, while the Nash index of the $\mathrm{SV_{OBS}}$ option was 34 % higher than the one of $\mathrm{COUPL_{MOD}}$ at Ners, the difference was only 6 % at Russan. Finally, for events no. 1 and 5, modelling with the $\mathrm{COUPL_{MOD}}$ option was much more satisfactory than with $\mathrm{SV_{OBS}}$. As already indicated (Sect. 4.2.2), the addition of lateral inflows was necessary for these two events. Some hydrographs obtained with the $\mathrm{SV_{OBS}}$ and $\mathrm{COUPL_{MOD}}$ options are provided in Fig. 7. Note the much better estimation of peak flow with $\mathrm{COUPL_{MOD}}$ for event no. 6. The index is 0.73 with $\mathrm{COUPL_{MOD}}$, and 0.77 with $\mathrm{SV_{OBS}}$.

5 Discussion

The presented results tend to justify the use of a coupling of models for a catchment like the Gardon river basin. However, several points can be discussed.

5.1 Concerning the choice of a hydraulic model based on full Saint-Venant equations

First of all, the choice of a hydraulic model based on full Saint-Venant equations can be questioned. Other simplified routing schemes would have been able to lead to equivalent results. Several studies inform the conditions of use of the simplifications of the dynamic equation that are the kinematic wave and the diffusive wave (Ponce et al., 1978; Daluz Vieira, 1983; Moussa and Bocquillon, 1996, 2000). Criteria, such the Froude number and the non-dimensionalised period characterizing the upstream initial condition (Moussa and Bocquillon, 1996), are used to define the domains of validity of these two schemes. In particular, it seems that the kinematic wave is well adapted to the areas where the river bed presents a slope of the order of 0.01 %, and to the areas where this slope is lower (of the order of 0.0001 %), but then in the limited case of slow floods (Ponce et al., 1978). The slopes of the Gardon, weak in the case of the reach studied (included between 0.001 and 0.003 %), and the speed of the floods, limit a priori its use. Furthermore, the kinematic wave, due to its simplifications, does not allow to reproduce the attenuation of the peak flows in the downstream part (Ponce et al., 1978; Keskin and Agiralioglu, 1997; Tsai, 2005), noticed on the Gardon river basin for events with essentially upstream rains. The diffusive wave option seems more attractive. Its use was validated for the Hérault river basin (France), close to the Gardon river and of equivalent area (Moussa and Bocquillon, 2009). However, as Moussa and Bocquillon (2000) notice it, its domain of validity is more restricted in the face of important flooded areas. Then, full Saint-Venant equations appear to be the ideal solution.

These remarks are to qualify by the fact that, as Hunter et al. (2007) note it, the modeling errors due to the specification of the topography and the values of the parameters (Ks), are often more important than those induced by the choice of a simplified model.

Another interesting alternative is the use of a hydrologic routing model with reservoirs. In the case of this study, the results of the LR model extended downstream are not satisfactory. However, the literature indicates performances close to those obtained with a hydraulic model based on full Saint-Venant equations, for a sophisticated version of the Muskingum scheme (O'Sullivan et al., 2012), or still for a lag-cascade routing model (Camacho and Lees, 1999). These options of improved hydrologic modellings can be interesting in the case of the Gardon river. Furthermore, it is possible that values of the V_0 and K_0 parameters of the LR model, directly adjusted on downstream reaches, rather than on the upstream *Gardon d'Anduze* river basin, provide better results. However, as Coustau (2011) indicates it, the SCS-LR model shows a sensibility more important for the S parameter with regard to these two routing parameters.

So, if a hydraulic model based on full Saint-Venant equations was chosen, other approaches seem possible on the scale of the Gardon river. Among these, the diffusive wave or improved hydrologic routing models, are interesting. However, other options, such the kinematic wave, are a priori to eliminate.

5.2 Concerning the parameters of the hydrologic models of sub-catchments

In this study, the parameters of the SCS-LR hydrologic model calibrated at Anduze are used for the others inflows of the hydraulic model, gauged (Alès), or not (48 lateral inflows). With this simplified approach, the performances of the coupling are satisfactory at the Ners, Russan and Remoulins stations. However, it can be improved, as is reflected by the differences in volumes observed between the downstream stations, with the volumes modelled for the lateral inflows included between these stations (Tab. 5), or the sometimes bad qualities noticed at the Alès station.

On this subject, the literature informs several options. Regionalization methods of model parameters were already experienced for numerous models and catchments

(Merz and Blöschl, 2004; McIntyre et al., 2005; Parajka et al., 2005; Oudin et al., 2008, 2010; Masih et al., 2010). These approaches consider criteria such as the spatial proximity, or still similarities between catchments (hydrological, geologic), to estimate the parameters adapted to the ungauged basin. Regressions between morphogeographical characteristics (for example the area, the averaged altitude or slope) and the calibrated parameters were also estimated. However, these regionalization methods are rather heavy, requiring an important quantity of data and processings because often experimented on a wide panel of catchments. Furthermore, most of the studies concern lumped models, a priori little adapted to the lateral inflows of the Gardon river basin.

More particularly, in Mediterranean basins, the research of Garambois (2012) or Artigue (2012) can be cited. Artigue (2012), working on ungauged catchments of the Gardon river, proposes a correction of the results of its neural networks model, by means of a relation based on the areas of the ungauged sub-catchments, and on the estimated maximal specific discharges. This strategy of correction allows for obtaining realistic modeled hydrographs. Garambois (2012) assesses regionalization methods of calibrated model parameters, for several sub-catchments of the Cevennes area. The author concludes that the similarity methods, defined from the characteristics of the ground, are particularly relevant.

These solutions constitute interesting ways to improve the hydrologic modellings of sub-catchments, and thus the results of the coupling of models.

6 Conclusions

This study showed that a coupling of hydrologic and hydraulic models is adapted for modelling the fast floods of the Gardon river basin. At the downstream stations of the catchment, the Nash values are included between 0.61 and 0.97, reflecting qualities rated as rather good to excellent. The coefficients specific to peak flows are also satisfactory. For the most part of the studied events, the relative error for peak flow (RE_{Qm})

is included between ±15 %, and the temporal difference (ΔT_{Qm}) is lower or of the order of 30 min. A comparison with other modelling strategies allows to estimate what improvements can be made to the coupling. Firstly, it seems that the choice of a hydraulic model based on full Saint-Venant equations to the routing in the downstream part of the Gardon river, is more appropriate than the LR hydrologic model. It would be advisable to complete this comparison with hydrologic routing models a little less simplistic, as for example the improved approach Muskingum (O'Sullivan et al., 2012), or with a hydraulic model based on the diffusive wave (Moussa and Bocquillon, 2009). Secondly, the interest of adding lateral inflows, as well as the impact of the qualities of the upstream inflows, were estimated. It emerges that adding lateral inflows improves modellings, of a way however variable according to the events. Only a case of degradation is observed (event no. 7, $\text{COUPL}_{\text{MOD}}$ vs. SV_{MOD}), and is understandable by an increase of the peak errors observed at Anduze and Alès. Also, the increase of the performances when the observed hydrographs at Alès and Anduze are used, depends on events. In these two cases, it seems that the cumulated rainfall spatial distribution plays an important role. When rains are concentrated in the upstream part of catchment, the good quality of modellings at upstream is essential. On the contrary, in the case of rains centered in the intermediary – downstream part of catchment, adding lateral inflows is necessary.

If the coupling results are satisfactory, they could be improved using better hydrological modellings of lateral inflows. On this subject, methods of correction of modellings (Artigue, 2012) or regionalization methods (Garambois, 2012), were analyzed for Mediterranean basins and seem relevant for this study case.

Finally, this coupling of models is very interesting for flood forecasting. In particular, it has a low number of adjustment parameters, S and V_0, parameters of the hydrologic model. In this study, they were calibrated, which is incompatible with a forecasting perspective. Recently, approaches of data assimilation for the estimation of these two parameters were developed and applied to the Lez river basin, in the south of France (Coustau, 2011; Coustau et al., 2013). The authors show that an assimilation in the first early hours of the flash flood allows to obtain a set of parameters providing good results. Other studies propose the use of indicators of initial state of the catchment to estimate a value of the *S* parameter for an upcoming event (Tramblay et al., 2010; Tramblay et al., 2011). The *Hu2* index of Météo-France, characterizing the initial humidity of the catchment, is particularly effective on the scale of the *Gardon d'Anduze*. These two methods, data assimilation or preliminary estimation by means of an indicator, completed by rainy forecasts, allow to envisage an employment of the coupling of models for flood forecasting at the Gardon river basin scale.

Acknowledgements. The authors thank Yann Laborda, from SPC-GD, for supplying the hydrological data useful to this study, and its sensible advice. Thanks are also presented to Fabrice Zaoui, from EDF, for its advice relating to the MASCARET code. Thanks to Guy Delrieu, from LTHE (*Laboratoire d'étude des Transferts en Hydrologie et Environnement*), to have supplied river cross sections, necessary for this study. Finally, thanks to Gilles Rocquelain, Fabrice Cebron and Marie-Christine Germain, from *BRL Ingénierie*, for their advice and remarks.

References

Anquetin, S., Braud, I., Vannier, O., Viallet, P., Boudevillain, B., Creutin, J.-D., and Manus, C.: Sensitivity of the hydrological response to the variability of rainfall fields and soils for the Gard 2002 flash-flood event, J. Hydrol., 394, 134–147, doi:10.1016/j.jhydrol.2010.07.002 2010.

Artigue, G.: Prévision des crues éclair par réseaux de neurones: généralisation aux bassins non jaugés, Ph. D., Université Montpellier II, Montpellier, France, 318 pp., 2012 (in French).

Artigue, G., Johannet, A., Borrell, V., and Pistre, S.: Flash flood forecasting in poorly gauged basins using neural networks: case study of the Gardon de Mialet basin (southern France), Nat. Hazards Earth Syst. Sci., 12, 3307–3324, doi:10.5194/nhess-12-3307-2012, 2012.

Ayral, P. A., Sauvagnargues-Lesage, S., and Bressand, F.: Contribution à la spatialisation du modèle opérationnel de prévision des crues éclair Alhtaïr, Études de Géographie Physique, 32, 75–97, 2005 (in French).

Biancamaria, S., Bates, P. D., Boone, A., and Mognard, N. M.: Large-scale coupled hydrologic and hydraulic modelling of the Orb river in Siberia, J. Hydrol., 379, 136–150, doi:10.1016/j.jhydrol.2009.09.054, 2009.

Bonnifait, L., Delrieu, G., Le Lay, M., Boudevillain, B., Masson, A., Belleudy, P., Gaume, E., and Saulnier, G. M.: Distributed hydrologic and hydraulic modelling with radar rainfall input: reconstruction of the 8–9 September 2002 catastrophic flood event in the Gard region, France, Adv. Water Res., 32, 1077–1089, doi:10.1016/j.advwatres.2009.03.007, 2009.

Bouvier, C., Marchandise, A., Lequien, A., Brunet, P., and Crespy, A.: Distributed rainfall/runoff modelling of September 2002 flood in two southern France river basins, BALWOIS International Scientific Conference, Ohrid, Republic of Macedonia, 25–29 May 2004, 2004.

Bouvier, C., Ayral, P. A., Brunet, P., Crespy, A., Marchandise, A., and Martin, C.: Recent advances in rainfall-runoff modelling: extrapolation to extreme floods in southern France, Proceedings of the AMHY-FRIEND International Workshop on Hydrological Extremes, University of Calabria, Cosenza, Italy, 3–4 May 2006, 229–238, 2006.

Braud, I., Roux, H., Anquetin, S., Maubourguet, M. M., Manus, C., Viallet, P., and Dartus, D.: The use of distributed hydrological models for the Gard 2002 flash flood event: analysis of associated hydrological processes, J. Hydrol., 394, 162–181, doi:10.1016/j.jhydrol.2010.03.033, 2010.

Camacho, L. A. and Lees, M. J.: Multilinear discrete lag-cascade model for channel routing, J. Hydrol., 226, 30–47, 1999.

Claudet, R. and Bouvier, C.: Outils de prévision des crues rapides: les besoins de l'alerte et du suivi en temps réel, Colloque SHF " Crues méditerranéennes", Nîmes, France, June 2004, 105–112, 2004 (in French).

Coustau, M.: Contribution à la prévision des crues sur le bassin du Lez: modélisation de la relation pluie-débit en zone karstique et impact de l'assimilation de débits, Ph. D., Université Montpellier II, Montpellier, France, 234 pp., 2011 (in French).

Coustau, M., Ricci, S., Borrell-Estupina, V., Bouvier, C., and Thual, O.: Benefits and limitations of data assimilation for discharge forecasting using an event-based rainfall–runoff model, Nat. Hazards Earth Syst. Sci., 13, 583–596, doi:10.5194/nhess-13-583-2013, 2013.

Daluz Vieira, J. H.: Conditions governing the use of approximations for the Saint-Venant equations for shallow water flow, J. Hydrol., 60, 43–58, 1983.

Delrieu, G., Ducrocq, V., Gaume, E., Nicol, J., Payrastre, O., Yates, E., Kirstetter, P. E., Andrieu, H., Ayral, P. A., Bouvier, C., Creutin, J. D., Livet, M., Anquetin, S., Lang, M., Neppel, L., Obled, C., Parent-du-Châtelet, J., Saulnier, G. M., Walpersdorf, A., and Wobrock, W.: The catastrophic flood event of 8–9 September 2002 in the Gard region, France: a first case study for the Cévennes-Vivarais Mediterranean Hydrometeorological Observatory, J. Hydrometeorol., 6, 34–52, 2005.

EDF-CETMEF: MASCARET v7.1 Note de principe, 152 pp., 2011.

Estupina-Borrell, V. and Dartus, D.: Evaluation of some rapid flood forecast models: TOPMODEL & MARINE, Transactions on Ecology and the Environment, 60, 45–54, 2003.

Garambois, P. A.: Étude régionale des crues éclair de l'arc méditerranéen français; élaboration de méthodologies de transfert à des bassins versants non jaugés, Ph. D., Université de Toulouse, Toulouse, France, 451 pp., 2012 (in French).

Gaume, E., Livet, M., Desbordes, M., and Villeneuve, J. P.: Hydrological analysis of the river Aude, France, flash flood on 12 and 13 November 1999, J. Hydrol., 286, 135–154, doi:10.1016/j.jhydrol.2003.09.015, 2004.

Hapuarachchi, H. A. P., Wang, Q. J., and Pagano, T. C.: A review of advances in flash flood forecasting, Hydrol. Process., 25, 2771–2784, doi:10.1002/hyp.8040, 2011.

Hunter, N. M., Bates, P. D., Horritt, M. S., and Wilson, M. D.: Simple spatially-distributed models for predicting flood inundation: a review, Geomorphology, 90, 208–225, doi:10.1016/j.geomorph.2006.10.021, 2007.

Jacq, V.: Inventaire des situations à précipitations diluviennes sur le Languedoc-Roussillon, la Provence-Alpes-Cote d'Azur, et la Corse – Période 1958–1994, Météo-France S3C/PRO, France, 190 pp., 1994 (in French).

Keskin, M. E. and Agiralioglu, N.: A simplified dynamic model for flood routing in rectangular channels, J. Hydrol., 202, 302–314, 1997.

Knebl, M. R., Yang, Z. L., Hutchison, K., and Maidment, D. R.: Regional scale flood modeling using NEXRAD rainfall, GIS, and HEC-HMS/RAS: a case study for the San Antonio River Basin summer 2002 storm event, J. Environ. Manage., 75, 325–336, doi:10.1016/j.jenvman.2004.11.024, 2005.

Lerat, J., Perrin, C., Andréassian, V., Loumagne, C., and Ribstein, P.: Towards robust methods to couple lumped rainfall-runoff models and hydraulic models: a sensitivity analysis on the Illinois River, J. Hydrol., 418–419, 123–135, doi:10.1016/j.jhydrol.2009.09.019, 2012.

Lian, Y., Chan, I. C., Singh, J., Demissie, M., Knapp, V., and Xie, H.: Coupling of hydrologic and hydraulic models for the Illinois River Basin, J. Hydrol., 344, 210–222, doi:10.1016/j.jhydrol.2007.08.004, 2007.

Manus, C., Anquetin, S., Braud, I., Vandervaere, J.-P., Creutin, J.-D., Viallet, P., and Gaume, E.: A modeling approach to assess the hydrological response of small mediterranean catchments to the variability of soil characteristics in a context of extreme events, Hydrol. Earth Syst. Sci., 13, 79–97, doi:10.5194/hess-13-79-2009, 2009.

Marchandise, A.: Modélisation hydrologique distribuée sur le *Gardon d'Anduze* ; étude comparative de différents modèles pluie-débit, extrapolation de la normale à l'extrême et tests d'hypothèses sur les processus hydrologiques, Ph.D. thesis, Université Montpellier II, Montpellier, France, 214 pp., 2007 (in French).

Martin, C.: Les inondations du 15 Juin 2010 dans le centre Var: réflexion sur un épisode exceptionnel, Études de Géographie Physique, 37, 41–76, 2010 (in French).

Masih, I., Uhlenbrook, S., Maskey, S., and Ahmad, M. D.: Regionalization of a conceptual rainfall-runoff model based on similarity of the flow duration curve: a case study from the semi-arid Karkheh basin, Iran, J. Hydrol., 391, 188–201, doi:10.1016/j.jhydrol.2010.07.018, 2010.

McIntyre, N., Lee, H., Wheater, H., Young, A., and Wagener, T.: Ensemble predictions of runoff in ungauged catchments, Water Resour. Res., 41, W12434, doi:10.1029/2005WR004289, 2005.

Mejia, A. I. and Reed, S. M.: Evaluating the effects of parameterized cross section shapes and simplified routing with a coupled distributed hydrologic and hydraulic model, J. Hydrol., 409, 512–524, doi:10.1016/j.jhydrol.2011.08.050, 2011.

Merz, R. and Blöschl, G.: Regionalisation of catchment model parameters, J. Hydrol., 287, 95–123, doi:10.1016/j.jhydrol.2003.09.028, 2004.

Montanari, M., Hostache, R., Matgen, P., Schumann, G., Pfister, L., and Hoffmann, L.: Calibration and sequential updating of a coupled hydrologic-hydraulic model using remote sensing-derived water stages, Hydrol. Earth Syst. Sci., 13, 367–380, doi:10.5194/hess-13-367-2009, 2009.

Moussa, R. and Bocquillon, C.: Criteria for the choice of flood-routing methods in natural channels, J. Hydrol., 186, 1–30, 1996.

Moussa, R. and Bocquillon, C.: Approximation zones of the Saint-Venant equations f flood routing with overbank flow, Hydrol. Earth Syst. Sci., 4, 251–260, doi:10.5194/hess-4-251-2000, 2000.

Moussa, R. and Bocquillon, C.: On the use of the diffusive wave for modelling extreme flood events with overbank flow in the floodplain, J. Hydrol., 374, 116–135, doi:10.1016/j.jhydrol.2009.06.006, 2009.

Moussa, R., Chahinian, N., and Bocquillon, C.: Distributed hydrological modelling of a Mediterranean mountainous catchment – model construction and multi-site validation, J. Hydrol., 337, 35–51, doi:10.1016/j.jhydrol.2007.01.028, 2007.

Nash, J. E. and Sutcliffe, J. V.: River flow forecasting through conceptual models part I – a discussion of principles, J. Hydrol., 10, 282–290, 1970.

Nelder, J. and Mead, R.: A simplex method for function minimization, Comput. J., 7, 308–313, 1965.

O'Sullivan, J. J., Ahilan, S., and Bruen, M.: A modified Muskingum routing approach for floodplain flows: theory and practice, J. Hydrol., 470–471, 239–254, doi:10.1016/j.jhydrol.2012.09.007, 2012.

Oudin, L., Andréassian, V., Perrin, C., Michel, C., and Le Moine, N.: Spatial proximity, physical similarity, regression and ungaged catchments: a comparison of regionalization approaches based on 913 French catchments, Water Resour. Res., 44, W03413, doi:10.1029/2007WR006240, 2008.

Oudin, L., Kay, A., Andréassian, V., and Perrin, C.: Are seemingly physically similar catchments truly hydrologically similar?, Water Resour. Res., 46, W11558, doi:10.1029/2009WR008887, 2010.

Parajka, J., Merz, R., and Blöschl, G.: A comparison of regionalisation methods for catchment model parameters, Hydrol. Earth Syst. Sci., 9, 157–171, doi:10.5194/hess-9-157-2005, 2005.

Ponce, V. M., Li, R. M., and Simons, D. B.: Applicability of kinematic and diffusion models, J. Hydr. Eng. Div.-ASCE, 104, 353–360, 1978.

Roux, H., Labat, D., Garambois, P.-A., Maubourguet, M.-M., Chorda, J., and Dartus, D.: A physically-based parsimonious hydrological model for flash floods in Mediterranean catchments, Nat. Hazards Earth Syst. Sci., 11, 2567–2582, doi:10.5194/nhess-11-2567-2011, 2011.

Ruin, I., Creutin, J. D., Anquetin, S., and Lutoff, C.: Human exposure to flash floods – Relation between flood parameters and human vulnerability during a storm of September 2002 in Southern France, J. Hydrol., 361, 199–213, doi:10.1016/j.jhydrol.2008.07.044, 2008.

Sangati, M., Borga, M., Rabuffetti, D., and Bechini, R.: Influence of rainfall and soil properties spatial aggregation on extreme flash flood response modelling: an evaluation based on the Sesia river basin, North Western Italy, Adv. Water Resour., 32, 1090–1106, doi:10.1016/j.advwatres.2008.12.007, 2009.

Saulnier, G. M. and Le Lay, M.: Sensitivity of flash-flood simulations on the volume, the intensity, and the localization of rainfall in the Cévennes-Vivarais region (France), Water Resour. Res., 45, W10425, doi:10.1029/2008WR006906, 2009.

Sauvagnargues-Lesage, S. and Simonet, C.: Retour d'expérience sur la gestion de l'évènement de Septembre 2002 par les Services de la Sécurité Civile, Houille Blanche, 6-2004, 1–7, 2004 (in French).

Thierion, V., Ayral, P. A., Geisel, J., Sauvagnargues-Lesage, S., and Payrastre, O.: Grid technology reliability for flash flood forecasting: end-user assessment, J. Grid Computing, 9, 405–422, 2011.

Toukourou, M., Johannet, A., Dreyfus, G., and Ayral, P. A.: Rainfall-runoff modeling of flash floods in the absence of rainfall forecasts: the case of "Cévenol flash floods", J. Appl. Intell., 35, 1078–1089, 2011.

Tramblay, Y., Bouvier, C., Martin, C., Didon-Lescot, J. F., Todorovik, D., and Domergue, J. M.: Assessment of initial soil moisture conditions for event-based rainfall-runoff modeling, J. Hydrol., 387, 176–187, doi:10.1016/j.jhydrol.2010.04.006, 2010.

Tramblay, Y., Bouvier, C., Ayral, P.-A., and Marchandise, A.: Impact of rainfall spatial distribution on rainfall-runoff modelling efficiency and initial soil moisture conditions estimation, Nat. Hazards Earth Syst. Sci., 11, 157–170, doi:10.5194/nhess-11-157-2011, 2011.

Tsai, C.: Flood routing in mild-sloped rivers – wave characteristics and downstream backwater effect, J. Hydrol., 308, 151–167, doi:10.1016/j.jhydrol.2004.10.027, 2005.

Whiteaker, T. L., Robayo, O., Maidment, D. R., and Obenour, D.: From a NEXRAD rainfall map to a flood inundation map, J. Hydrol. Eng., 11, 37–45, doi:10.1061/(ASCE)1084-0699(2006)11:1(37), 2006.

Zoccatelli, D., Borga, M., Zanon, F., Antonescu, B., and Stancalie, G.: Which rainfall spatial information for flash flood response modelling? A numerical investigation based on data from the Carpathian range, Romania, J. Hydrol., 394, 148–161, doi:10.1016/j.jhydrol.2010.07.019, 2010.

Table 1. Drained areas and outlet distances for the five stations.

Stations	Drained areas (km^2)	Outlet distances (km)
Anduze	545	83.7
Alès	315	81.7
Ners	1100	64.3
Russan	1530	45.3
Remoulins	1900	13.9

Table 2. Some key event characteristics. AN, N, and RU stand for the Anduze, Ners, and Russan stations. UP groups together both upstream sub-catchments (Anduze and Alès).

Event	Period	Mean rainfall (mm)			Runoff volume (Mm^3)			Peak discharge (m^3 s^{-1})		
		UP	N	RU	UP	N	RU	AN	N	RU
1	5–12 Sep 2005	280	300	320	–	63	99	150	460	850
2	18–22 Oct 2006	210	170	140	–	91	85	1300	1340	1290
3	21–24 Oct 2008	190	180	160	46	52	50	1070	1390	1340
4	1–4 Nov 2008	250	230	190	98	118	113	1040	1290	1420
5	6–9 Sep 2010	90	120	140	2	15	21	20	560	700
6	21–28 Dec 2010	160	150	130	97	126	133	360	730	880
7	2–9 Nov 2011	460	430	370	195	222	229	1070	1120	1300

Title Page
Abstract Introduction
Conclusions References
Tables Figures
◀| |▶
◀ ▶
Back Close
Full Screen / Esc
Printer-friendly Version
Interactive Discussion

Table 3. S and V_0 parameters calibrated at the Anduze station, for the seven events studied.

Event	S	V_0
1	391	1.6
2	238	3.6
3	408	3.1
4	203	3
5	367	1.4
6	108	1.6
7	227	2.7

Table 4. Performance indices at the Anduze and Alès stations.

Event	Anduze			Alès		
	Nash	RE_{Qm}	ΔT_{Qm}	Nash	RE_{Qm}	ΔT_{Qm}
1	0.72	−11	−15	–	–	–
2	0.87	−10	10	–	–	–
3	0.91	−25	5	0.89	2	25
4	0.90	−20	−5	0.57	−3	25
5	0.53	−6	−5	−4.57	17	30
6	0.68	15	705	−0.50	24	45
7	0.80	−15	1415	−0.25	69	1180

NHESSD
1, 4635–4680, 2013

A coupling of models appropriate for the Gardon river basin

O. Laganier et al.

Table 5. Comparison of the differences in volumes (Mm^3) observed between stations (V_{OBS}), and lateral inflow volumes estimated with SCS-LR ($V_{SCS\text{-}LR}$), in both sections Anduze/Alès (UP) – Ners and Ners – Russan.

Event	UP – Ners		Ners – Russan	
	V_{OBS}	$V_{SCS\text{-}LR}$	V_{OBS}	$V_{SCS\text{-}LR}$
1	–	15.0	35.7	39.9
2	–	0.2	0	0.2
3	5.6	2.4	0	0
4	19.4	5.1	0	1.2
5	12.9	9.2	5.7	11.1
6	28.9	7.5	6.4	6.3
7	27.7	18.2	7.1	19.4

Table 6. Performance indices at the Ners, Russan and Remoulins stations.

Event	Ners			Russan			Remoulins
	Nash	RE_{Qm}	ΔT_{Qm}	Nash	RE_{Qm}	ΔT_{Qm}	ΔT_{Qm}
1	0.77	−23	−30	0.86	1	−260	−210
2	0.61	4	25	0.72	−4	5	20
3	0.92	3	15	0.97	−3	10	10
4	0.80	1	−20	0.86	−11	−35	−25
5	0.68	−30	−15	0.88	−12	−20	−10
6	0.64	0	90	0.73	−11	55	70
7	0.75	39	1270	0.79	15	1275	1300

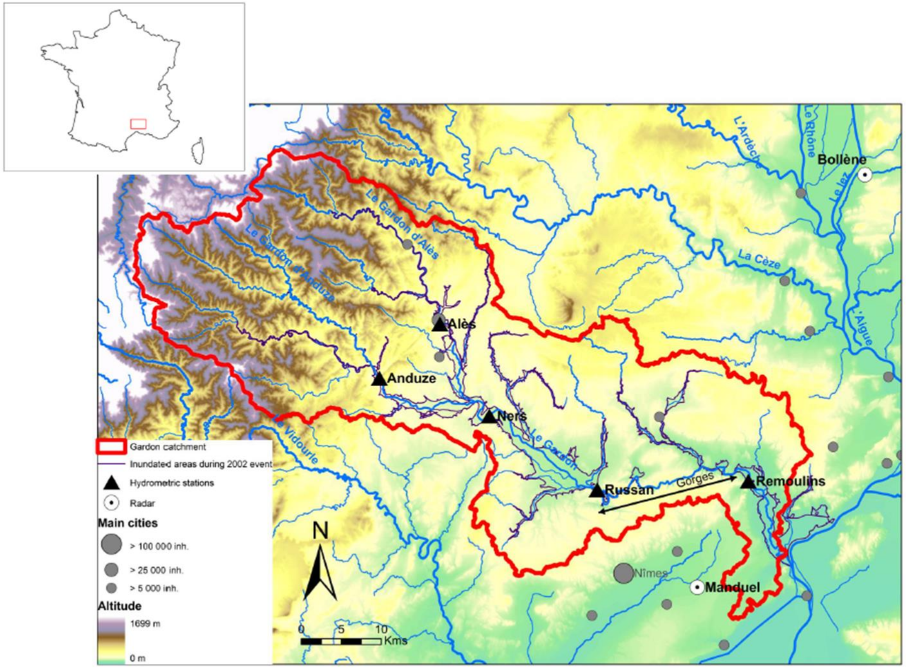

Fig. 1. The Gardon catchment.

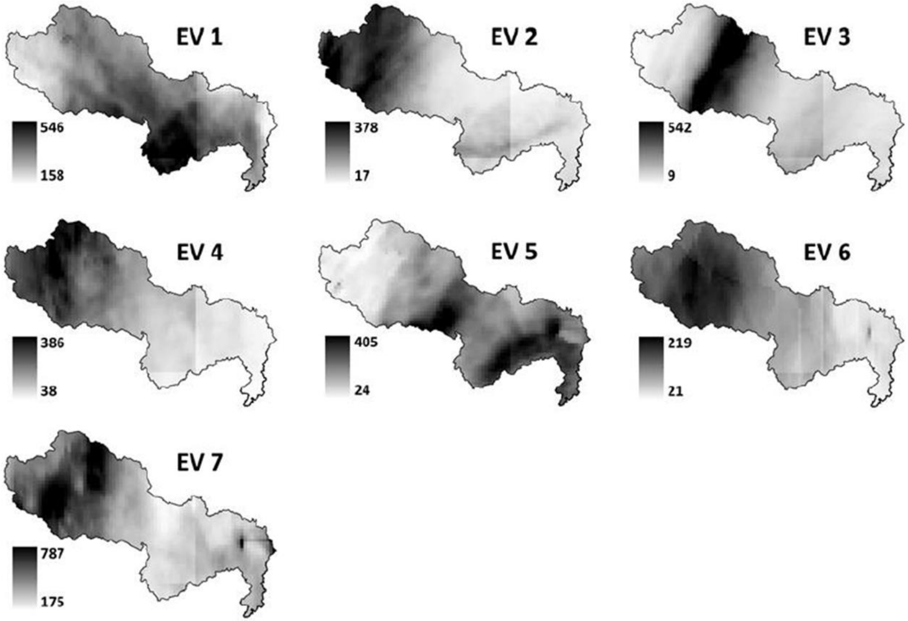

Fig. 2. Cumulated rainfall (mm) for each event.

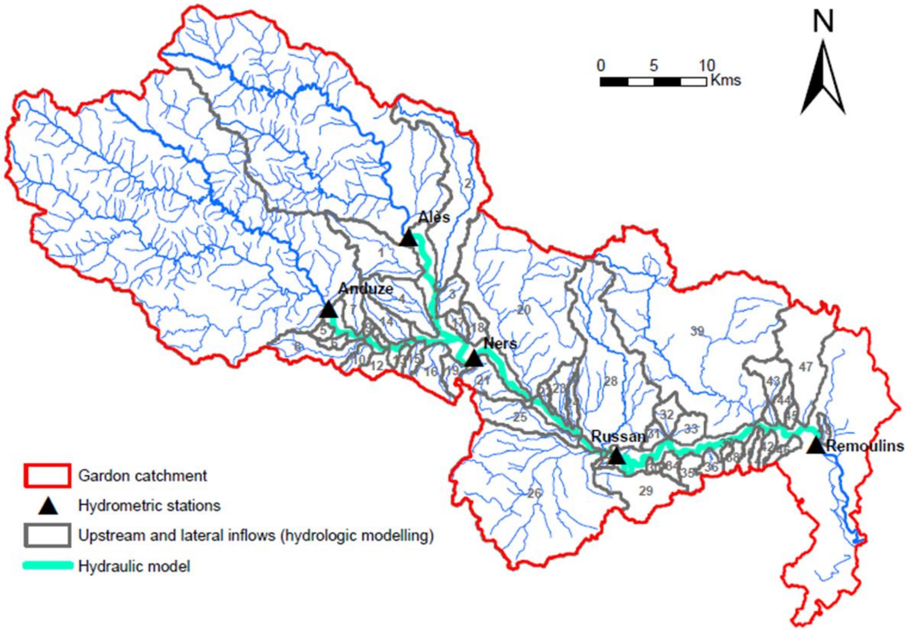

Fig. 3. Coupled models applied to the Gardon river basin.

Title Page
Abstract
Introduction
Conclusions
References
Tables
Figures
◀I
▶I
◀
▶
Back
Close
Full Screen / Esc
Printer-friendly Version
Interactive Discussion

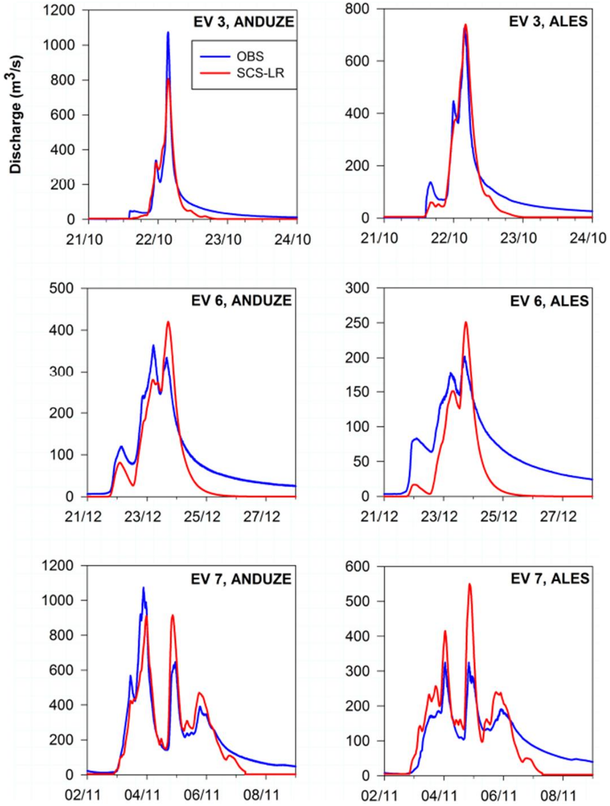

Fig. 4. Hydrographs modelled (with SCS-LR) for events no. 3, 6, and 7 at the Anduze and Alès stations ($m^3\,s^{-1}$).

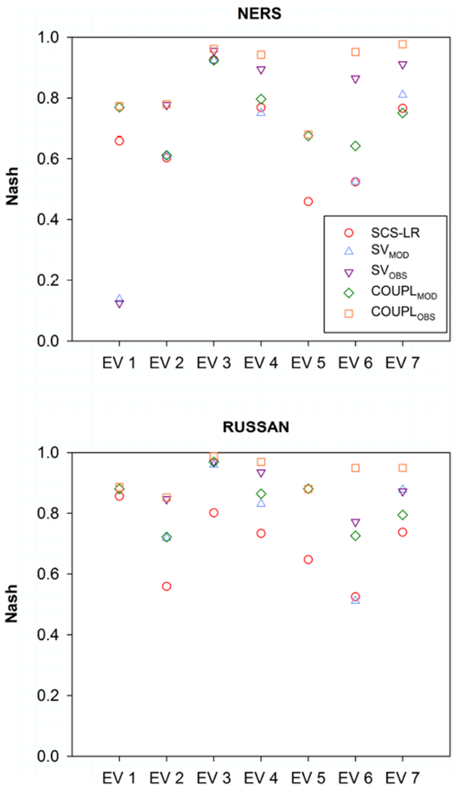

Fig. 5. Nash values according to the different modelling options, at the Ners and Russan stations.

NHESSD
1, 4635–4680, 2013

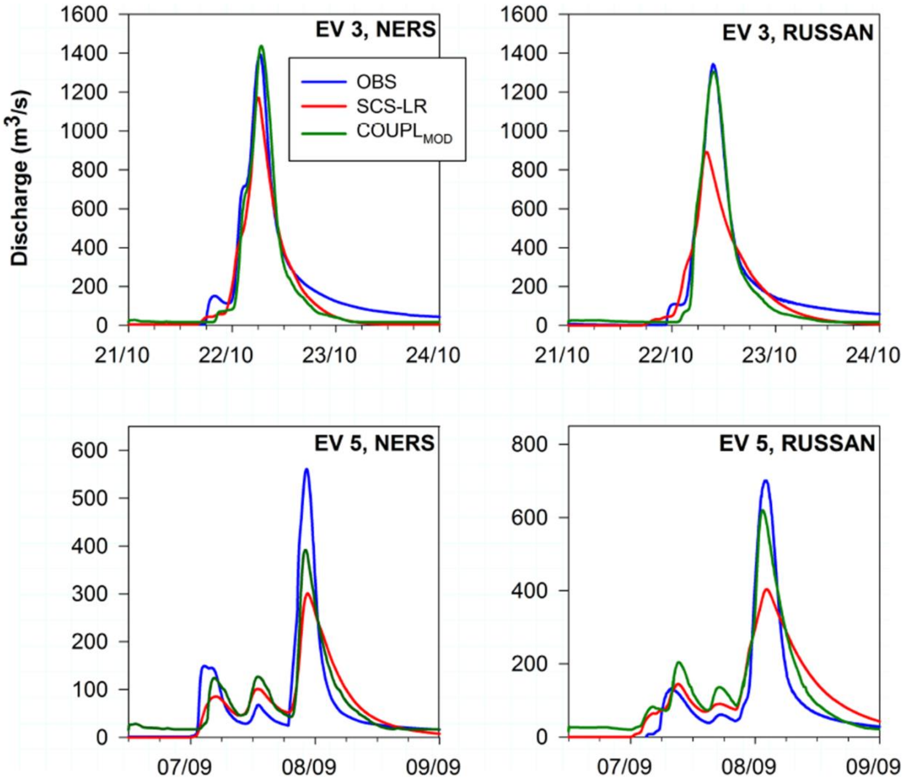

Fig. 6. Hydrographs modelled for events no. 3 and 5 according to SCS-LR and COUPL$_{MOD}$ modelling options, at the Ners and Russan stations (m^3 s^{-1}).

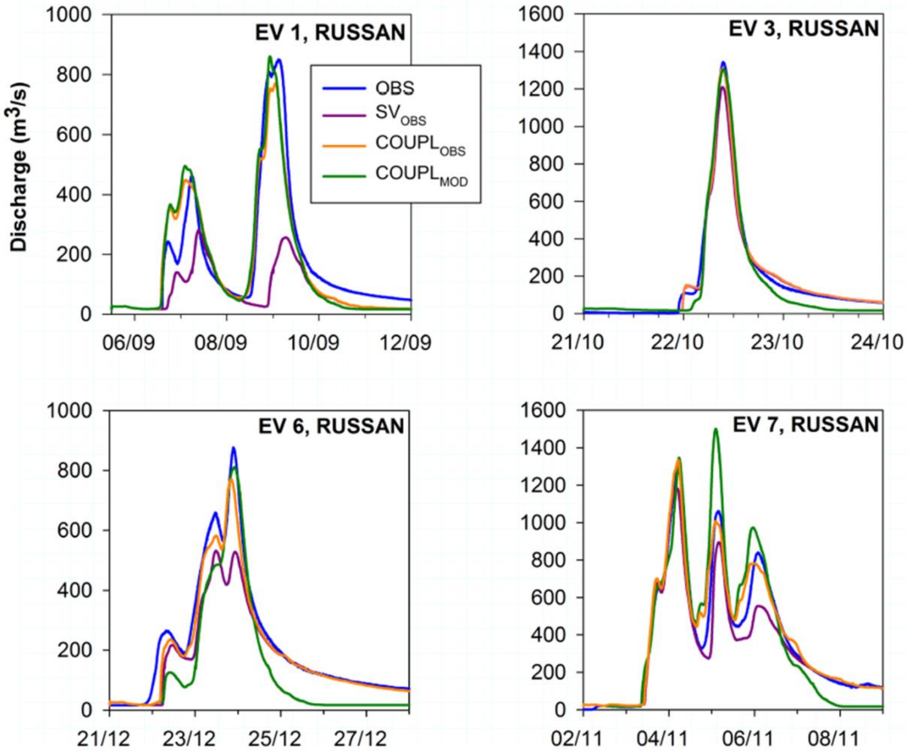

Fig. 7. Hydrographs modelled for events no. 1, 3, 6 and 7 according to SV_{OBS}, $COUPL_{OBS}$ and $COUPL_{MOD}$ modelling options, at the Russan station ($m^3\,s^{-1}$).